Aggregation phenomena in a system of molecules with two internal states

R. Gaspari, A. Gliozzi, and R. Ferrando
Dipartimento di Fisica and INFM, Via Dodecaneso 33, Genova, I16146, Italy
(Received 5 July 2007; revised manuscript received 1 September 2007; published 19 October 2007)

A model for the aggregation of molecules with two internal states is studied by kinetic Monte Carlo simulations. Molecules are represented by simple beads, discarding all stereochemical specificity. Monomers are placed in a three-dimensional lattice and diffusion processes are simulated, as well as internal state conversions of the molecules. The two internal states feature a stable (S) not assembly competent configuration, and an unstable assembly competent (A) configuration. Monomers in A state are given a higher energy if isolated, but they can reach the lowest energy level through short-range interactions between each other, so that their aggregation is promoted. Kinetics of cluster formation are examined, as well as the basic mechanisms ruling growth in our system. The simulations show that the aggregation process is preceded by a lag phase, which is followed by a fast growth phase. The duration of the lag phase is determined by the strength of the A-A interaction, whereas the time slope of the growth phase is mainly influenced by the conversion rate between internal states. The whole work has been inspired by the biological problem of amyloid aggregation, whose aggregation curves often present a sigmoidal behavior which is reproduced by the present model.

DOI: 10.1103/PhysRevE.76.041604 PACS number(s): 81.10.Aj, 68.55.Ac, 81.10.Dn

I. INTRODUCTION

Cluster growth science has gained increased attention over the past few years, as it has proved fundamental to outlining the physical basis that lies is below the preparation of materials on the nanometer scale. Nano-objects are very interesting both for industrial applications and theoretical research. In order to understand the wide range of phenomena that refer to nanoscience, growth kinetics of nanosized structures must be investigated. Traditionally, solid state physics has focused on growth of metallic clusters and crystals, thus providing a rich variety of tools for experimental investigation and theoretical analysis in this field [1,2]. Numerical simulation has yielded valuable results in the development of microscopic theory and has successfully reproduced experimentally observed phenomena on realistic time scales. They have often used kinetic Monte Carlo (KMC) methods together with simplified descriptions of space geometry to describe nonequilibrium growth phenomena such as kinetic roughening and molecular beam epitaxy growth [1,3,4].

In this paper we take advantage of these approaches to simulate the self-assembly phenomena of nanometer-sized particles in solution, thus mimicking a general process of growth for molecules on this length scale. These particles (referred to as monomers in the following) can alternatively occupy two states, depending on their internal configuration. State S is stable and not assembly competent, i.e., particles in state S do not have tendency to form aggregates. State A is metastable and assembly competent, as monomers in this state can interact through a short-range attractive potential. A cubic lattice is used to schematize the tridimensional solvent and short-range attractive forces have been modeled as first neighbor interactions, by following the example of many other condensed matter simulations ruled by KMC algorithms [1,5,6]. The model used in this work takes into account a variety of events, including adsorption and desorption processes, monomer and cluster diffusion.

Despite being quite general, our model has been inspired by the problem of amyloid aggregation [7–11], where small biological units (being either proteins or small peptides), whose hydrodynamic radius is in the nanometer scale, can be modeled as an ensemble of molecules with two internal states, displaying the properties of our A-S beads [11–15]. These polypeptides, in fact, can lose their native, correctly folded conformation by assuming a misfolded structure, unfavored in bulk solution. This behaviour might be explained by the hypothesis that amyloid proteins have a double funnel potential energy surface (PES) [11,16–18]. In this case, one of these funnels could act as a kinetic trap for misfolded polypeptides, with misfolding-refolding time depending on the energetic barriers between the minima corresponding to the two different structures. Amyloid protein PES is also more complicated if we consider intermolecular interactions between polypeptides. In this case, a still deeper minimum could appear as a result of interactions between misfolded proteins [14] (Fig. 1), thus explaining the great stability of amyloid assemblies [7,8]. All these aspects can be considered in our simulations as A beads might be referred to as misfolded polypetides while S beads can correspond to the soluble, native proteins. Even though a realistic description of amyloid aggregate geometry goes well beyond the aim of the simple approach proposed here, our paper may therefore serve as a basis for a deeper understanding of these systems using the tools of statistical mechanics.

In our simulations, we monitor the kinetics of cluster growth and observe a sigmoidal time dependence of growth-related parameters. The sigmoidal behavior is a consequence of a nucleation process, and consists of a lag phase, in which no significant aggregation takes place, followed by a rapid growth phase. The sigmoidal behavior is common in experiments of protein aggregation *in vitro* [19–22].

We have therefore studied the effects of changing some of the parameters of the system, such as the interaction energies and the relative stability of monomers, on typical aggregation times, namely lag-phase time and growth rate. Great attention has been paid in understanding the features of the lag phase of the systems. Actually, sudden changes of system properties happens at the end of the lag phase, when one or

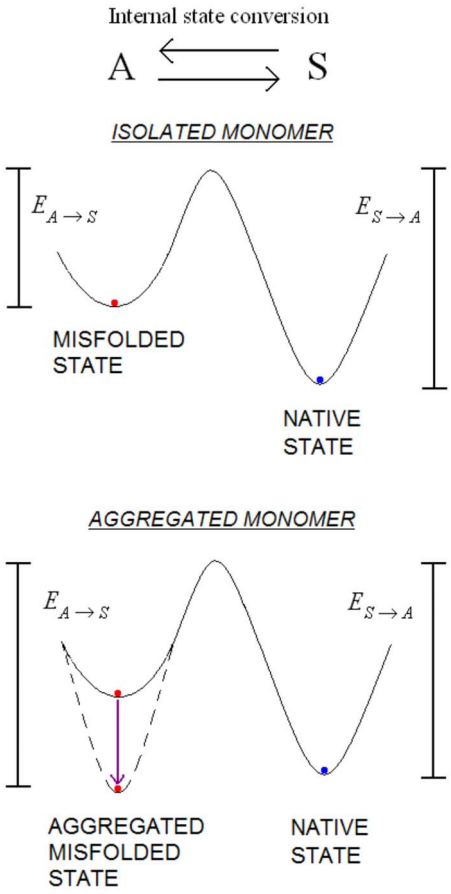

FIG. 1. (Color online) Schematic representation of the model PES of a molecule with two internal states. (a) PES for isolated monomers: A state is higher in energy. (b) PES for interacting monomers: A state lowers its energy and becomes the lowest minimum.

more clusters join a threshold (*critical*) structure and a rapid growth begins. An extended investigation covering the aspects of critical structures is reported in a separate section of this paper.

The paper is structured as follows. Section II contains the description of the model and of the computational methodology. Section III reports the results of our simulation in dependence of model parameters, and the study of nucleation processes. Finally, Secs. IV and V contain the discussion of the results and the conclusions, respectively.

II. MODEL AND METHODS

In our model we consider a cubic lattice with periodic boundary conditions, where each lattice site can be either occupied by a monomer in A or S state or by a solvent unit. Type A monomers form a bond when they are first neighbors while S monomers only interact through excluded volume forces. Monomer energies are defined as follows: S monomers are given a 0 energy level by default; the energy of an A monomer varies as follows:

$$E_{\mathrm{A}} = E_{\mathrm{A}}^{0} - nE_{\mathrm{A\text{-}A}}, \tag{1}$$

where n is the coordination number (i.e., the number of first-neighbor A monomers), E_{A}^{0} is the energy for an isolated A monomer, and $E_{\mathrm{A\text{-}A}}$ is the interaction energy per bond.

Monomers can either diffuse in a first neighbor solvent site or convert their internal state (mimicking a misfolding-refolding process if referred to an amyloid protein ensemble). When an assembly of monomers forms, so that all its components can be connected to each other by an on-lattice pathway excluding solvent sites, that assembly will be registered as a cluster unit. Cluster units can diffuse through a uniform translation of all cluster components by a single lattice spacing.

All events take place in the system at their specific rate constant, which are of Arrhenius form. For a process k rate R_k is given by

$$R_k = \nu_k \exp\left(-\frac{E_k}{k_{\mathrm{B}}T}\right), \tag{2}$$

where ν_k is the prefactor, E_k is the activation barrier, k_{B} is the Boltzmann costant, and T is the temperature.

In order to quantify event rates it will be necessary to sort out energetic barriers and frequency prefactors for all processes. For diffusion processes, the knowledge of the monomer coordination number is sufficient to get energy barrier values. In fact, in our model, energy barriers equal monomer binding energy as far as single monomer diffusion processes are concerned [23]. This means that the diffusion rate of isolated monomers between neighbor sites sets our elementary time scale. Similarly, energy barriers are set to 0 for cluster diffusion as this event requires no bonds to be destroyed.

The barriers for internal conversion processes are chosen as follows (see Fig. 1). For A monomers the conversion barrier changes with the coordination number as follows:

$$E_{\mathrm{A}\to\mathrm{S}} = E_{\mathrm{A}\to\mathrm{S}}^{0} + nE_{\mathrm{A\text{-}A}}, \tag{3}$$

where $E_{\mathrm{A}\to\mathrm{S}}^{0}$ is the activation barrier for internal conversion of an isolated A monomer. In the case of S monomers, the conversion barrier $E_{\mathrm{S}\to\mathrm{A}}$ has a unique value, given by $E_{\mathrm{S}\to\mathrm{A}}=E_{\mathrm{A}\to\mathrm{S}}^{0}+E_{\mathrm{A}}^{0}$. In writing Eqs. (1) and (3), we assume that the energy of state A is lowered by the bonding to nearest-neighbor monomers, while the energy of the saddle point for the $\mathrm{A}\to\mathrm{S}$ conversion and vice versa is left unaltered.

A single prefactor $\nu=1/\tau$ is chosen for all processes. In the following, times will be measured in units of τ, unless otherwise specified. Diffusion rates of clusters are chosen to scale inversely with their size [24].

Event selection is decided by a KMC method using a searching algorithm which uses two binary trees. The first binary tree is used to search through events concerning monomers, while the second is used to search through events concerning clusters. In order to choose which binary tree is to be searched, the algorithm extracts a random number r in the range $[0, R_{cl}+R_{mon}]$ where R_{cl} is the sum of all event rates concerning clusters and R_{mon} is the sum of all event rates concerning monomers. If $r<R_{mon}$, then the binary tree concerning monomers will be chosen, otherwise the binary tree concerning clusters will be selected. After this choice event, selection is made by going down the binary tree cho-

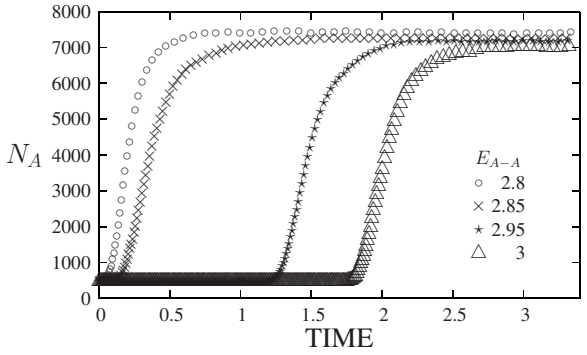

FIG. 2. Growth profiles from four different simulations, all showing a sigmoidal shape. N_A is the number of monomers in state A. The curves are obtained from simulations at different values of monomer interaction $E_{A\text{-}A}$ by keeping conversion barrier $E^0_{A\to S}$ fixed at 2. The main effect of varying interaction energies is a substantial change of the lag-phase time. Time is measured in units of $10^5\tau$.

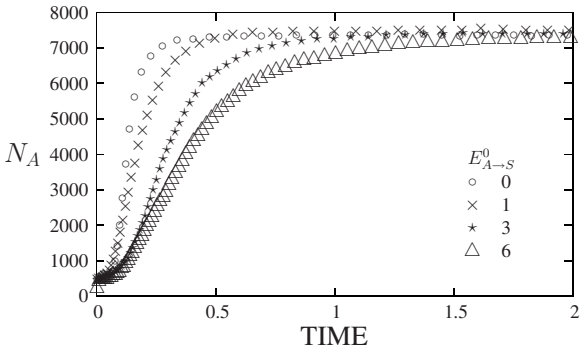

FIG. 3. Growth profiles from four different simulations. N_A is the number of monomers in state A. The curves are obtained from simulations at different values of the conversion barrier $E^0_{A\to S}$ by keeping monomer interaction energy $E_{A\text{-}A}$ fixed at 3. The main effect of varying activation barriers for conversion is a change of the curve slope during the growth phase. Time is measured in units of $10^5\tau$.

sen as usual for binary tree searching alghoritms [25]. An equivalent choice could be to combine both trees in a single binary tree containing all possible events. Also, time step choice is made as usual for KMC methods [26,27]. Unless otherwise stated, some system parameters are kept constant in the simulations discussed in the next section. Our lattice is a cubic box of $64\times64\times64$ sites with periodic boundary conditions containing 8192 monomers, the equivalent of a 3.125% lattice sites. In the following, energies are measured in units of k_BT, where T is fixed. An isolated A monomer has an energy $E^0_A=3$. The initial configuration of the system is set so that monomers are randomly distributed in space and are all in S state. If referring to amyloid growth problem, this would mean that we want to monitor how a whole set of native proteins can evolve before aggregation and growth phenomena eventually appear.

By fixing the above parameters, the system configuration will be completed by choosing $E_{A\text{-}A}$ and $E^0_{A\to S}$, so that we will mainly discuss how growth kinetics are affected from a change in their values.

III. RESULTS

A. Effects of parameters $E_{A\text{-}A}$ and $E^0_{A\to S}$ on aggregation kinetics

Here we show typical growth profiles by plotting the number of A monomers in solution against time. These kinds of curves display well the aggregation state of the system since, as will be better discussed later, cluster growth determines a raise in the number of A particles. The common hallmark for all these curves is the sigmoidal profile. This is a quite interesting feature, as these kinds of profiles are also typical of *in vitro* amyloid aggregation [19–22], when optical properties related to aggregation in the protein systems are plotted against time.

We can distinguish four different phases in the sigmoidal growth profiles seen in our simulations. There is an initial equilibration, where the A monomers number increases from 0 to the value proper of the subsequent lag phase. In the lag phase, the number of A monomers fluctuates close to its statistical value in the absence of aggregation (which can be readily deduced from Boltzmann distribution). Then a growth phase follows, in which one or more clusters rapidly expand. Finally, there is a saturation phase with no further growth.

The first phase is often not clearly visible in the curves shown in this section. In fact, points in the curves describing this phase are very few, as every single point is averaged over millions of steps, and correspond to a small span of time if compared to the whole simulation time. Anyway, the initial transient appears more clearly when conversion state barriers become higher. In Figs. 2 and 3 we show a comparison of results obtained by varying one of the parameters of the system ($E_{A\text{-}A}$ and $E^0_{A\to S}$, as discussed in Sec. II), the others being kept fixed. The comparison indicates a clear role of the different parameters on typical aggregation times of the system. Our results indicate that the lag phase becomes longer as the interaction energy parameter is lowered (Fig. 2), while the growth rate decreases when conversion state

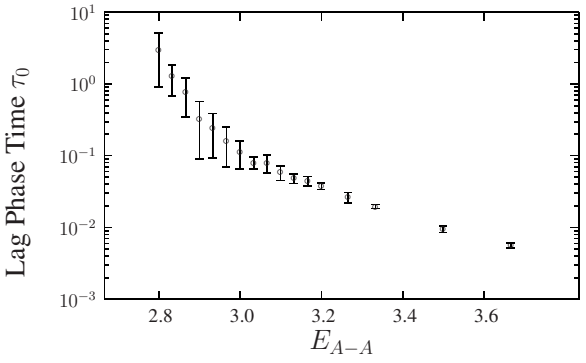

FIG. 4. Dependence of the lag-phase time τ_0 on monomer interaction energy $E_{A\text{-}A}$. Energy is in k_BT units, lag-phase time $10^5\tau$ units. The conversion barrier $E^0_{A\to S}$ is kept fixed at 2. Data are averaged over 10 independent simulations.

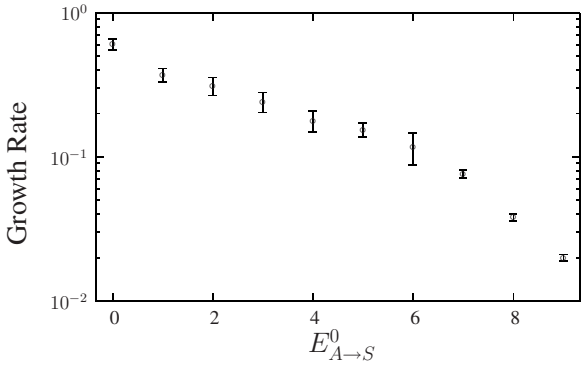

FIG. 5. Dependence of the growth rate on the conversion barrier $E^0_{\mathrm{A}\to\mathrm{S}}$. Energy is in $k_\mathrm{B}T$ units, growth rate in monomers/τ. The interaction energy $E_{\mathrm{A\text{-}A}}$ is kept fixed at 3. Data are averaged over 10 independent simulations.

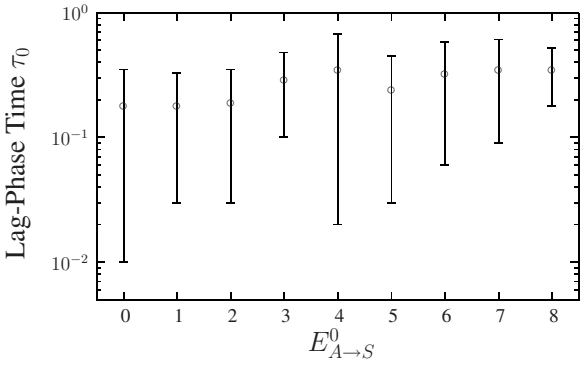

FIG. 7. Dependence of the lag-phase time τ_0 on the conversion barrier $E^0_{\mathrm{A}\to\mathrm{S}}$. Energy is in $k_\mathrm{B}T$ units, lag-phase time is in $10^5\tau$ units. The interaction energy $E_{\mathrm{A\text{-}A}}$ is kept fixed at 2.9. Data are averaged over ten independent simulations.

barriers are raised (Fig. 3). To quantify the dependence of the typical aggregation times on system parameters, averages over ten independent simulations for each parameter set were made. In Figs. 4–7, we show the dependence of the lag-phase time and of the growth rate on $E_{\mathrm{A\text{-}A}}$ and $E^0_{\mathrm{A}\to\mathrm{S}}$. The growth rate is computed as the slope of the growth phase in the region where A monomers are between 1500 and 3000 units. Lag-phase time is calculated from the intercept of growth phase linear fit and lag phase plateau. Results confirm a very strong dependence (more than exponential) of the lag-phase time on $E_{\mathrm{A\text{-}A}}$, and a remarkable dependence of the growth rate on $E^0_{\mathrm{A}\to\mathrm{S}}$. In addition to this, it can be noticed that growth rate depends on $E_{\mathrm{A\text{-}A}}$ until a saturation value is reached; that clearly defines a diffusion limited regime. By contrast, changes in $E^0_{\mathrm{A}\to\mathrm{S}}$ do not seem to greatly affect lag-phase times.

In the following we analyze in more detail the results obtained with two specific parameter sets.

(a) *Weakly interacting A particles*: $E_{A\text{-}A}=2.8$, $E^0_{A\to S}=2$. In Fig. 8, a growth profile is shown. In this case the lag-phase time extends over a significant span of time, in which no evident aggregation phenomena take place. The lag phase is characterized by continuous aggregation and dissolution of small-size oligomers that do not survive for long in solution as interaction energies are weak. By contrast, the end of the lag phase is due to the formation of an oligomeric nucleus overcoming a threshold critical structure. This critical assembly rapidly grows for inclusion of A monomers coming on its surface from bulk solution. Growth is characterized by continuous rearrangement of A monomers on surface kinks, so that growing clusters reach subsequent squared, compact structures. Due to depletion effects, growth slows down as the cluster expands, and lastly ends in a saturation phase, where bulk monomers reach and leave the cluster surface at the same rate.

(b) *Strongly interacting A particles*: $E_{\mathrm{A\text{-}A}}=4$, $E^0_{\mathrm{A}\to\mathrm{S}}=2$. A completely different scenario appears by slightly raising $E_{\mathrm{A\text{-}A}}$. In this case the lag phase is dramatically reduced and growth phenomena appear consequently to the expansion of several nuclei. Figures 9 and 10 show how temporal evolution changes just by raising interaction energy to four units. The lag phase completely vanishes and clusters undergo fast expansion on a much shorter time scale. Also, cluster geometry varies remarkably if compared to that obtained at lower

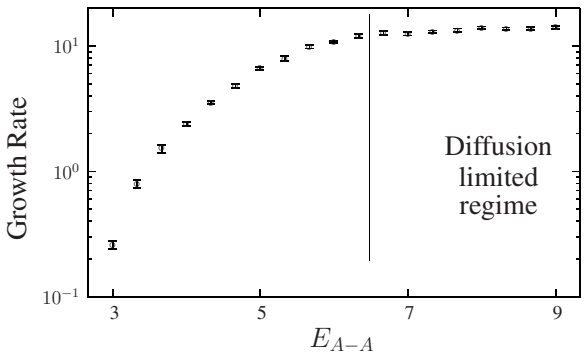

FIG. 6. Dependence of the growth rate on monomer interaction energy $E_{\mathrm{A\text{-}A}}$. Energy is in $k_\mathrm{B}T$ units, growth rate in monomers/τ. The conversion barrier $E^0_{\mathrm{A}\to\mathrm{S}}$ is kept fixed at 2. Data are averaged over 10 independent simulations. A diffusion-limited regime is found for large $E_{\mathrm{A\text{-}A}}$ values.

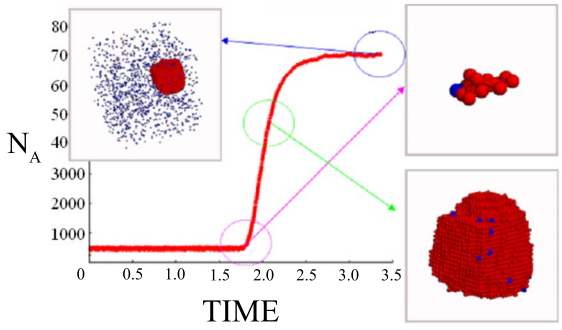

FIG. 8. (Color online) Typical sigmoidal shape of the growth profile. The number of A monomers N_A is reported as a function of time (measured in $10^5\tau$ units). The two images on the right depict the clusters with more than five monomers. The image corresponding to the end of simulation reports a snapshot of the whole system. Red (light gray) spheres are A monomers while blue (dark gray) spheres are S monomers.

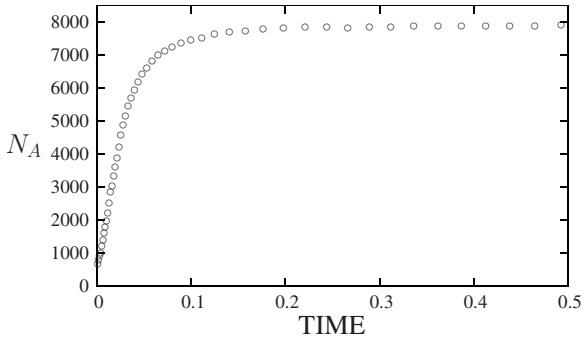

FIG. 9. The number of A monomers N_A as a function of time is registered during a simulation at $E_{A\text{-}A}=4$ and $E^0_{A\to S}=2$. Time is in units of $10^5\tau$. No lag phase is detected.

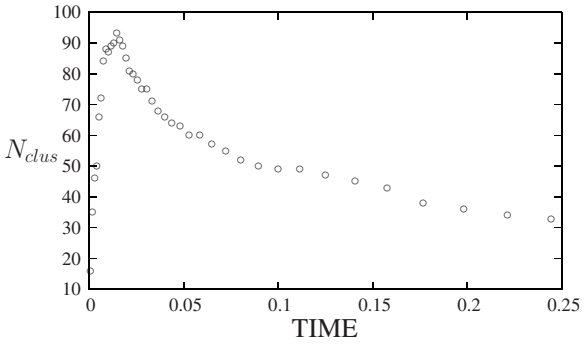

FIG. 10. The number of clusters containing more than five monomers (N_{clus}) is reported as a function of time in the case of the simulation reported in Fig. 9. Time is in units of $10^5\tau$. There is a peak in the cluster number during the growth phase, followed by a decrease in the saturation phase due to cluster colliding and merging.

interaction energies. As reported in Fig. 11, a high number of nuclei keep growing and merging during both growth and saturation phases, so that very irregular clusters are found at the end of the simulation.

B. Comparison with the results in two dimensions

It is indeed interesting to know whether a sigmoidal growth profile can be seen when the model is simulated in two dimensional (2D). To answer this question we have performed a simulation in a 2D lattice (512×512 sites) with no change to other system parameters as specified in Sec. II. We have been able to observe a sigmoidal profile also in this case, as shown by Fig. 12. Indeed, some differences with regard to the 3D case must be pointed out: while in the 3D case we are able to see a clear sigmoidal profile when $E_{A\text{-}A}$ is set between 3.0 and 2.8 (lower values of $E_{A\text{-}A}$ give such long time lags that exceed our computational capabilities), this range appears to be shifted in the 2D case, so that we can see the sigmoidal profile when $E_{A\text{-}A}$ is set between 3.5 and 3.3. Moreover, in 2D space, the saturation phase is reached for much smaller clusters than in 3D space. These features can be explained by taking into account the difference of physics in 2D and 3D space. The main aspect to highlight is that, in the 2D case, a monomer can form up to four bonds, against the six bonds of the 3D case. Therefore, a monomer in a kink position in 3D space is more bounded than it would be in 2D, provided interaction energies are the same in both cases. Interaction energies in 2D have then to be tuned properly if we want to reproduce the lag times of the 3D case. The smaller number of bonds being formed together with different surface/volume ratio of clusters are then responsible for a different behavior of growth in 2D. These aspects have to be taken into account when considering system properties, such as equilibrium size of clusters and their growth rate.

C. Study of the nucleation process

As shown previously, the lag phase ends when one or more oligomers reach a given threshold critical structure, and the growth phase begins. In order to study nuclei critical structure in a quantitative way, we have developed a simplification of the model previously described, so as to gain a better view of the essential nucleation mechanisms, and a quicker way to accumulate statistics on the results obtained.

In this approximation we simulate the growth of a single cluster in solution. This can be useful if one wants to single out the mechanisms that rule cluster growth in solution as only adsorption and desorption events are taken into account. In this approximation a small oligomer (it can also be a single monomer) is placed randomly on the lattice and is subject to the mean conditions it would experience in bulk solution. For simplicity, this oligomer is made by A monomers only. Growth will also be referred to the inclusion of an A monomer on the cluster surface. Cluster surface is meant

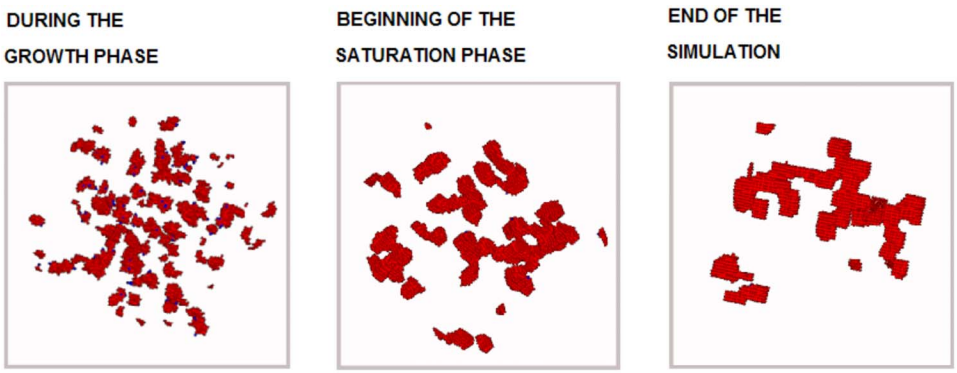

FIG. 11. (Color online) View of the system at three different stages in the case of the simulation reported in Fig. 9. Only the clusters made of more than five monomers are shown.

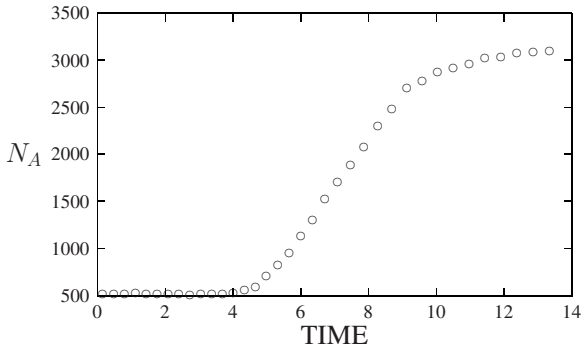

FIG. 12. Sigmoidal shape of the growth profile for the 2D model, in the case of $E_{\text{A-A}}=3.4$ and $E^0_{\text{A}\to\text{S}}=2$. Time is given in units of $10^5\tau$. N_{A} is the number of monomers in state A.

as the number of solvents sites that are first neighbors to any component of the cluster. The oligomer can therefore grow for two main reasons: the diffusion of an A monomer from bulk solution on cluster surface; the state conversion of an S monomer deposited on cluster surface. Similarly the cluster can reduce its size for two reasons: the diffusion of an A state monomer away of the cluster surface; the state conversion of a cluster component that is first neighbor to at least one solvent site. Processes that can take place in this simplified model are random deposition on cluster surface and monomer detachment from cluster edges. In this way, we are able to model nucleation and understand what phenomena are taking place during the lag phase; however, this simplified model cannot account for the slope of the growth phase, which is mainly ruled by the interconversion rate between A and B monomers.

The mean growth rate R_{in}, taking into account the contributions described earlier, is obtained with the aid of simple statistical mechanics reasonings:

$$R_{in} = \frac{S}{N_{sol}}(N_{\text{A}}K^0_{diff} + N_{\text{S}}K_{\text{S}\to\text{A}}), \tag{4}$$

where S is the surface extension, N_{sol} is the total number of solvent sites, N_{A} and N_{S} are the total number of monomers in A and S, state respectively, K^0_{diff} is the diffusion rate for isolated A monomers, $K_{\text{S}\to\text{A}}$ is the conversion rate for S monomers. The number of A monomers is given by its equilibrium value in absence of aggregation (so as to approach the number of A monomers during the lag phase).

Similarly the mean escape rate for monomer k, $R_{k,out}$, is given by

$$R_{k,out} = (6 - l_k - d_k)K_{k,diff} + K_{k,\text{A}\to\text{S}}, \tag{5}$$

where l_k is the number of bonds, d_k is the total number of surface diffusion directions on cluster surface, $K_{k,diff}$ is the diffusion constant, and $K_{k,\text{A}\to\text{S}}$ is the conversion rate for monomer k.

Events selection is ruled by a KMC algorithm in the following way. A random number r is chosen in the range $[0, R_{in}+R^{TOT}_{out}]$, where R^{TOT}_{out} is the sum of the desorption rates of all monomers belonging to the cluster. If $r<R^{TOT}_{out}$, a desorption event is selected following the KMC rules, otherwise a random deposition on cluster surface is performed.

System parameters are chosen in the same way as described in Sec. II. This is a simplified model since it does not take into account the effects of cluster local concentration that increases as monomers diffuse away from the cluster edges. In fact, these monomers are considered as emitted in bulk solution, without taking into account their proximity with the cluster itself. Cluster collision contribution to growth is also discarded and surface diffusion is only taken into account by the d_k factor in Eq. (5), so that explicit migration of monomers along the cluster surface is not considered. As a consequence, results obtained within this approximation will differ from those obtained under the same conditions in the full simulation. Nevertheless, the approach presented in this section can help us to provide an insight on the general features of growth phenomena from solution, by providing a simple scenario where cluster properties can be inferred by comparison of corresponding R_{in} and R^{TOT}_{out}. In the following we shall present the results obtained within this model.

The abrupt and sudden change of system features is due to nucleation-dependent processes. It is therefore interesting to investigate what size must be joined by a cluster before starting rapid growth. In order to get more insight we have used the simplified model described earlier for monitoring the mechanism of growth of a single cluster. Cluster structures with $R_{in}>R_{out}$ have been monitored during cluster growth. These structures are quite interesting as they allegedly promote growth to larger assemblies. We will label these structures as metastable. On the contrary, structures with $R_{out}>R_{in}$ are unstable. Often a metastable structure (i.e., cubic octamer) becomes unstable by simple addition of a low-coordination monomer on its surface. In Fig. 13 we show the results of a simulation performed with a single monomer put in solution at $t=0$. The sizes of metastable structures have been registered as a function of the number of simulation steps. A zoom in three different regions is reported in order to have a better view of growth mechanisms. Figure 13 shows that the cluster grows and dissolve many times before a critical nucleus is formed, at least when interaction energies are not set too high. By zooming in on the figure in the regions A, B, C, one has a better view of growth mechanisms. These regions show that cluster structures oscillate around some peculiar configuration before changing size. For example, zoom B of Fig. 13 shows that the cluster oscillates many times around a structure of eight units (easily identified as a cubic octamer by comparison with other data). This particular feature is also seen in zoom C which depicts cluster growth after a critical nucleus has formed. It is clear from this picture that also growth after the formation of a critical nucleus is characterized by several oscillations around metastable configurations. A question that may arise is therefore the following: which is the critical size of a nucleus? In other words, what is the size a cluster should join so that it does not completely dissolve anymore? To answer this question we have put several structures in solution at the first step of simulation, at different interaction energies. We then performed one hundred simulations per structure at the different energies assessed. The structures studied are shown in Fig. 14. Table I shows that there is a number of structures

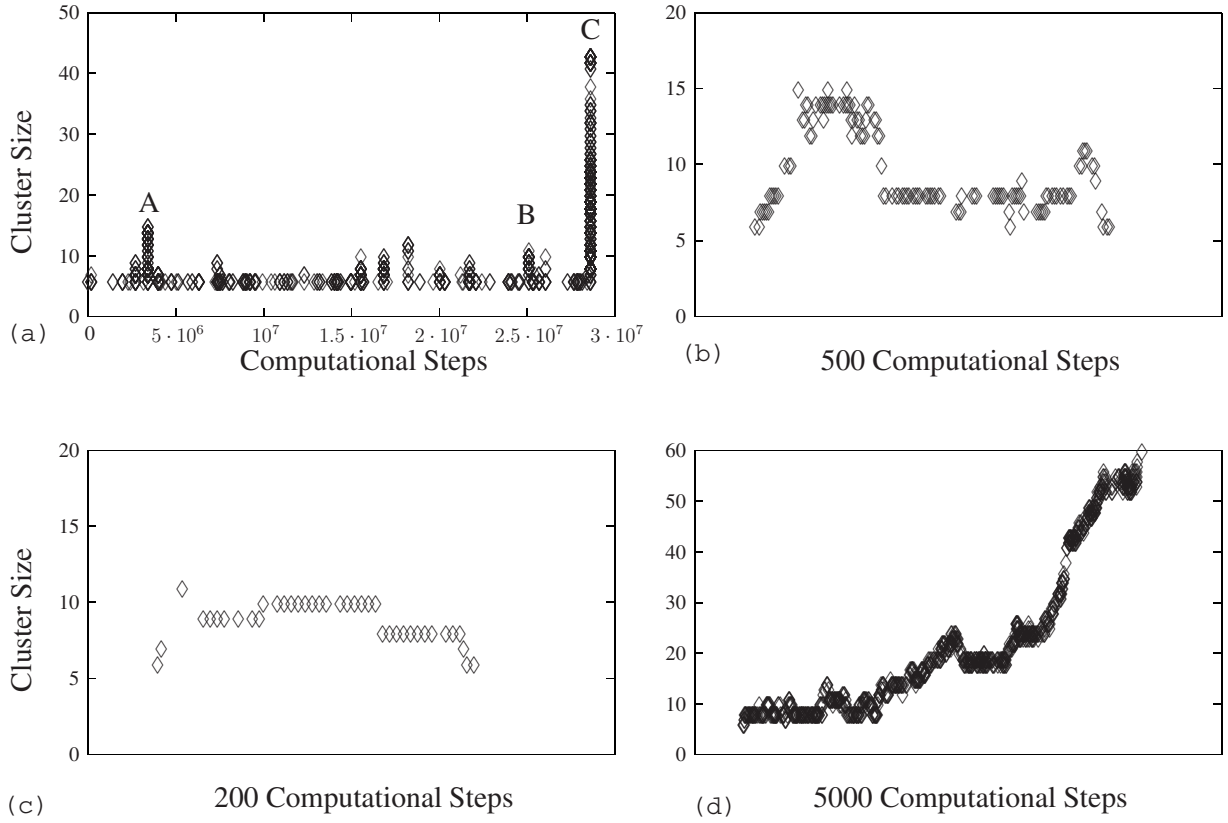

FIG. 13. Top left panel: cluster size as a function of time (measured in computational steps) for the simplified model in which a single cluster is growing. Each point in the graph corresponds to a metastable structure encountered during time evolution. Model parameters are $E_{A\text{-}A}=3.3$ and $E^{0}_{A\rightarrow S}=2$. Several metastable structures are encountered before the final growth towards a large aggregate. (b) and (c) show zooms around the peaks indicated by A and B in part (a). These zooms show that several metastable structures form and dissolve. (d) shows a zoom of the curve at the beginning of the final growth phase.

that, once formed, can either completely disrupt or indefinitely grow. These structures have a certain probability of being the critical nuclei; this probability is strongly dependent on the interaction energy. In fact, for $E_{A\text{-}A}=3.4$, a double layer of 3×3 squared islets is already sufficient for promoting fast growth in 96% of cases. Decreasing interaction energy by 0.2 only makes the probability of fast growth of this structure to drop to 45%.

IV. DISCUSSION

Sigmoidal growth profiles are indeed related to a nucleation process. When the system rests in the lag phase, monomers diffuse and collide so as to form small oligomers. These oligomers, once formed, can either grow or lose monomers, as our model takes into account adsorption and desorption events at their specific rates. Results of simulations within

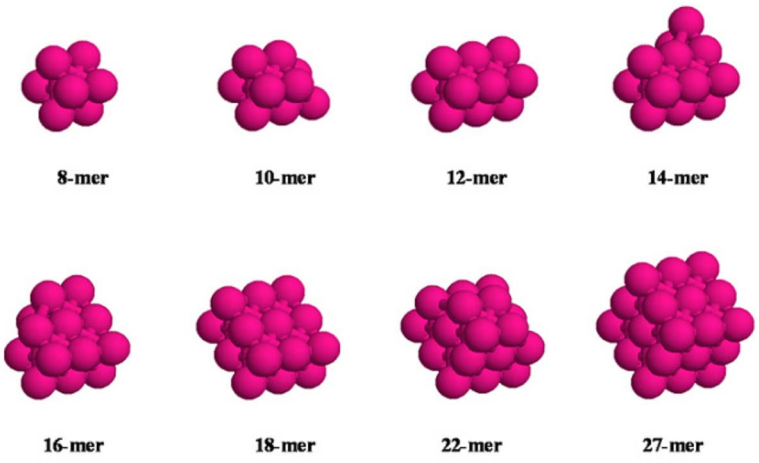

FIG. 14. (Color online) A sample of metastable structures is displayed: starting from the cubic octamer, structures until 18-mer are obtained by addition of a dimer on cluster surface. The 22-mer is obtained by adding a tetramer on the 18-mer surface.

TABLE I. Survival probabilities of aggregates of different initial sizes at three values of $E_{A\text{-}A}$. In the first column we report the initial size of the aggregate. N_{dis} is the number of times that the aggregate dissolves in 100 simulations. N_{gro} is the number of times that the aggregate grows to very large sizes in 100 simulations.

$E_{A\text{-}A}\rightarrow$	3.4		3.3		3.2	
Size ↓	N_{dis}	N_{gro}	N_{dis}	N_{gro}	N_{dis}	N_{gro}
8	90	10	99	1	100	0
10	83	17	96	4	100	0
12	66	34	80	20	98	2
14	9	91	40	60	67	33
16	4	96	18	82	45	55
18	0	100	3	97	16	84
22	0	100	0	100	0	100

the simplified model, as displayed by Fig. 13, show that a certain number of oligomers has to form and completely dissolve before a critical nucleus forms and fast growth is triggered. Exceptions take place at very high interaction energies where desorption events are almost absent and growth can be considered as irreversible. Continuous creation and dissolution of clusters during the lag phase is then a common hallmark for systems with low interaction energies. It is indeed of primary importance in determining typical lag-phase times. In fact, when by chance one of these oligomers reaches a given size, it can become a critical nucleus and undergo fast expansion. Thus the lag phase quickly comes to an end. It must be noticed anyway that a unique definition of critical nucleus for the systems investigated is quite difficult, as the geometry of clusters varies considerably and many assemblies can display the features of a critical nucleus. This observation agrees with the results obtained with the simplified model, where a number of structures have undergone a rapid growth after being put in solution at the first step of the simulation. Indeed, many of them were on the brink of criticality, as they displayed both the characteristics of unstable dissociating oligomers and of critical nuclei at almost the same amount. The way oligomers form and then become critical assemblies is the key point in understanding the mechanisms of growth in our systems. In order to get a detailed description of cluster growth, the importance of metastable structures must be noted. In fact, results reported in Fig. 13 show that clusters can oscillate around metastable structures many times before growing to a bigger metastable conformation or being degraded to a smaller one. Oscillations have to be meant as repeated adsorption and desorption of a few monomers upon a metastable structure (for example, continuous desorption and adsorption of a low coordinated monomer on a cubic 8-mer cluster). The number of oscillation steps a cluster can hold in solution without disruption to a smaller metastable structure can be considered as its mean lifetime or the time it has to attempt new and bigger metastable configurations. Clusters in expansion have therefore to rush their way through metastable structures without lodging on any of them for a time longer then their mean lifetime. If a cluster fails to do this it will be degradated to a smaller structure. If it happens at the early stage of cluster formation (below critical size) this process can take a cluster back to its monomeric form. If it happens when clusters are beyond the critical size, a disruption process can take place anyway, but it never causes the full dissociation of the cluster, as the chances to run the complete way back to its monomeric form are statistically irrelevant. Let us try to quantify what we have said so far by considering the 8-mer of Fig. 14, at $E_{A\text{-}A}=3.2$. The probability that, in a couple of subsequent simulation steps, a cubic 8-mer grows to a metastable 10-mer by addition of a dimer on one of its faces is given as follow:

$$P_{growth}^{8^*\rightarrow 10^*} = P_{growth}^{8^*\rightarrow 9^*} P_{growth}^{9^*\rightarrow 10^*}, \tag{6}$$

where asterisks are used to differentiate metastable structures. Probability of growth from an 8-mer to a 9-mer is

$$P_{growth}^{8^*\rightarrow 9} = \frac{R_{in,8^*}}{R_{in,8^*} + R_{out,8^*}}. \tag{7}$$

Probability of growth from the 9-mer to the 10-mer is

$$P_{growth}^{9\rightarrow 10^*} = \frac{R_{in,9}}{R_{in,9} + R_{out,9}} \frac{N_{k,9}}{S_9}, \tag{8}$$

where $N_{k,9}$ is the number of kinks and S_9 is the surface of the 9-mer. The probability of monomer escape from a cubic 8-mer is:

$$P_{growth}^{8^*\rightarrow 7^*} = \frac{R_{out,8^*}}{R_{in,8^*} + R_{out,8^*}}. \tag{9}$$

By substituting numerical values one obtains that the value given by Eq. (9) is higher than that given by Eq. (6). So, nucleation of a new layer upon a face of the cubic 8-mer is unfavored. Similar calculations show that, under the same conditions, nucleation on a cubic 27-mer is favored, thus explaining part of the results of Table I. This reasoning can be applied to understand a variety of situations. Results of our simulations show that the interaction energy strongly affects lag-phase times. This is due to two different reasons: on one hand, results obtained with the simplified model show that the size of the critical nucleus is highly dependent on the interaction energy. On the other hand, on-pathway intermediate oligomers are less stable at low $E_{A\text{-}A}$, thus increasing the time required for nuclei formation. Once a nucleus has formed, its expansion can be very fast if compared to the lag-phase time. Conversion state barriers play a major role in determining the slope of the growth phase (see Fig. 5) while they have little impact on the lag-phase time. This feature can be explained by thinking that, after a nucleus has formed, its growth rate depends on the amount of A monomers adsorbed on its surface per unit time. The number of A monomers in bulk solution decreases as a result of their adsorption on growing clusters and, if conversion barriers are high, replacement in bulk solution can be very slow, thus affecting the rate of incoming A monomers on cluster surface. Nevertheless, also interaction energies can have an impact on the growth rate, even though their main effect is on the lag-phase time. This effect is explained by the nature of

growth in our system: in fact, clusters above the critical size can also partly dissociate, by oscillating a certain number of times around peculiar structures. These oscillations can be reduced through higher interaction energies, speeding up growth. This effect has been quantified in Fig. 6 for high interaction energies. When $E_{\text{A-A}}$ is raised above a threshold level, the growth rate becomes independent of $E_{\text{A-A}}$ and diffusion limited. It is reasonable to think that the diffusion limited regime is reached when $E_{\text{A-A}}$ is sufficient to make the dimer a metastable structure. The threshold energy for this to happen, under the conditions in which the curve in Fig. 6 has been obtained, can be readily calculated by setting $E_{\text{A-A}}$ so that $R_{in}-R_{out}^{TOT}=0$ for dimers. Calculation yields a threshold energy of about 6.6, in agreement with results obtained by simulations, as shown by Fig. 6. By contrast, lag-phase times are not affected by the energetic barrier $E_{\text{A}\to\text{S}}^{0}$ as reported by Fig. 7. This is reasonable since the lag phase of any system can be roughly considered as the equilibrium phase when $E_{\text{A-A}}=0$. Thermodynamic properties of a system can only depend on monomer energy so that the energetic barrier $E_{\text{A}\to\text{S}}^{0}$ cannot affect the lag-phase time. At the end of growth phase, the rate of A monomer adsorption on clusters in solution equals the rate of monomer dissociation from clusters and this equilibrium is the cause for saturation phase. During the saturation phase, anyway, cluster shape continues to change by rearranging its components in order to reach more compact and low energy dispositions.

Finally, we note that the simplified model presented in this section provides results that are suitable to comparison with classical theory of growth. This theory predicts that formation of a critical cluster requires an expense of free energy ΔG^{*} and that nucleation rate J can be written as

$$J \propto e^{-\Delta G^{*}}. \tag{10}$$

ΔG^{*} can be written, using an atomistic approach [28] as

$$\Delta G^{*} = -n^{*}\Delta\mu + \Phi, \tag{11}$$

where n^{*} is the number of monomers in the critical nucleus, $\Delta\mu$ is the supersaturation (i.e., the difference between the chemical potential of the solid and the vapor phase), and Φ is the surface energy of the growing cluster (i.e., the number of uncompensated bonds of cluster monomers). Using the atomistic approach to nucleation phenomena, an expression of supersaturation in terms of our system parameters can be roughly found to be [28]

$$\Delta\mu = \frac{2E_{\text{A-A}}}{(n^{*})^{1/3}}. \tag{12}$$

By considering that surface energy should scale as surface extension [i.e., $\propto(n^{*})^{2/3}$], rearranging terms in Eq. (11) and taking the reciprocal of nucleation rate as lag-phase time (τ_0) we have

$$\log\tau_0 \propto (n^{*})^{2/3}. \tag{13}$$

In order to verify this dependence we proceed as follows. First, for each nucleus size we determine the energy $E_{\text{A-A}}$ at which that nucleus is critical. It has been assumed that a cluster is critical at a given energy when its survival probability overcomes 95% (see Table I for examples). Then, we determine the average lag-phase time as a function of $E_{\text{A-A}}$. Twenty simulations within the simplified model are performed for each energy in order to have a fair statistical accuracy in lag-phase times evaluation. The data in Fig. 15 agree well with the dependence proposed in Eq. (13). From our data, however, we cannot exclude other dependencies, as also a linear dependence $\log(\tau_0)\propto n^{*}$ fairly fits our results, even though with less accuracy than Eq. (13).

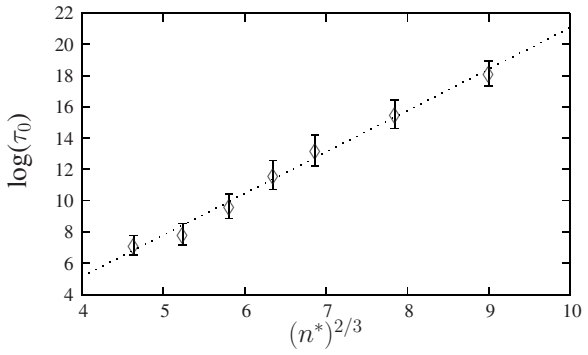

FIG. 15. Logarithm of the lag-phase time τ_0 as a function of $(n^{*})^{2/3}$, where n^{*} is the size of the critical nucleus. τ_0 is measured in units of computational steps. The data accommodate well on a straight line, in agreement with Eq. (13).

V. CONCLUSIONS

In this work we developed a simple model of aggregation of molecules whose energy landscape can be described, in a coarse-grained way, by two different internal states, A and S. The model has been studied by means of kinetic Monte Carlo simulations. Our basic approach can provide insight on the general features of these ensembles and can be easily extended to the description of more specific situations, provided one has reliable information on activation barriers and temporal prefactors. The A-S duality of the nature of monomers can be referred to as an amyloid protein ensemble. Though much more detail is required to get any realistic information on precursor assembly kinetics of amyloid deposits, our results suggest that sigmoidal growth profiles are typical not only of amyloid assemblies, but of a wide range of systems of molecules with two possible configurations, the first stable and interacting with simple excluded volume forces, the second unstable and able to form short-range reversible bonds. This in turn highlights the nucleation-dependent nature of growth in these systems.

ACKNOWLEDGMENTS

The authors acknowledge financial support from a grant by Fondazione CARIGE, and are grateful to A. Relini and R. Rolandi for useful discussions.

[1] M. Kotrla, Comput. Phys. Commun. **97**, 82 (1996).
[2] F. Baletto and R. Ferrando, Rev. Mod. Phys. **77**, 371 (2005).
[3] A.-L. Barabasi and H. E Stanley, *Fractal Concepts in Surface Growth* (Cambridge University Press, Cambridge, U.K., 1995).
[4] O. Trushin, A. Karim, A. Kara, and T. S. Rahman, Phys. Rev. B **72**, 115401 (2005).
[5] J. Marro and R. Dickman, *Nonequilibrium Phase Transitions in Lattice Models* (Cambridge University Press, Cambridge, U.K., 1999).
[6] C.-Y. Yang, W. Y. Shih, and W.-H. Shih, Phys. Rev. E **64**, 021403 (2001).
[7] M. Stefani, Biochim. Biophys. Acta **1739**, 5 (2004).
[8] E. Zerovnik, Eur. J. Biochem. **269**, 3362 (2002).
[9] C. M. Dobson, Semin Cell Dev. Biol. **15**, 3 (2004).
[10] J. W. Kelly, Curr. Opin. Struct. Biol. **8**, 101 (1998).
[11] J. W. Kelly, Nat. Struct. Biol. **7**, 824 (2000).
[12] T. Scheibel, J. Bloom, and S. L. Lindquist, Proc. Natl. Acad. Sci. U.S.A. **101**, 2287 (2004).
[13] P. Gorbenko and K. J. Kinnunen, Chem. Phys. Lipids **141**, 72 (2006).
[14] F. E. Cohen and S. B. Prusiner, Annu. Rev. Biochem. **67**, 793 (1998).
[15] T. R. Serio, A. G. Cashikar, A. S. Kowal, G. J. Sawicki, J. J. Moslehi, L. Serpell, L. M. F. Arnsdorf, and S. L. Lindquist, Science **289**, 1317 (2000).
[16] J. P. K. Doye, A. Miller, and D. J. Wales, J. Chem. Phys. **110**, 6869 (1998).
[17] P. L. Clark, TIBS **29**, 527 (2004).
[18] D. J. Wales, *Energy Landscapes with Applications to Clusters, Biomolecules and Glasses* (Cambridge University Press, Cambridge, U.K., 2003).
[19] W. Koo and D. Miranker, Protein Sci. **14**, 231 (2005).
[20] B. Padrick and D. Miranker, Biochemistry **41**, 4694 (2002).
[21] R. F. Pasternack, E. J. Gibbs, S. Sibley, L. Woodard, P. Hutchinson, J. Genereux J, and K. F. Kristian, Biophys. J. **90**, 1033 (2006).
[22] D. Hamada and C. M. Dobson, Protein Sci. **11**, 2417 (2002).
[23] A. Danani, R. Ferrando, E. Scalas, and M. Torri, Surf. Sci. **409**, 117 (1998).
[24] P. Jensen, Rev. Mod. Phys. **71**, 1695 (1999).
[25] A. Videcoq, F. Hontinfinde, and R. Ferrando, Surf. Sci. **515**, 575 (2002).
[26] K. Fichthorn and W. H. Weinberg, J. Chem. Phys. **95**, 1090 (1991).
[27] A. F. Voter, F. Montalenti, and T. C. Germann, Annu. Rev. Mater. Res. **32**, 321 (2002).
[28] I. Markov, *Crystal Growth for Beginners* (World Scientific Publishing, Singapore, 1995), Chap. 2.2.